A Configuration of Double Input Z-Source DC-DC Converter for Standalone PV/Battery System Application

Farzad Sedaghati[1], **Shamim Mohammad Salehian**[2], **Hossein Shayeghi**[3], **and Elias Shokati Asl**[4]

[1, 2, 3, 4] *Department of Electrical and Computer Engineering, Faculty of Engineering, University of Mohaghegh Ardabili, Ardabil, Iran*
[*] *Corresponding author: farzad.sedaghati@uma.ac.ir*

Manuscript received 31 March, 2018;Revised 22 May, 2018, accepted 28 August,2018. Paper no. JEMT-1803-1069.

In this paper, a double input DC-DC converter based on modified Z-source converter is suggested for standalone PV/Battery system application. The configuration of double input DC-DC converter under one port powered off is presented to solve problem of randomness and intermittency in distributed power source. In the proposed topology, the input DC voltage is boosted and achieved higher voltage gain with lower voltage stress on power switches. Other merits of the proposed converter are that it operates with wide range of load, and input DC voltage sources supply DC load individually or simultaneously. The configuration of the proposed double input DC-DC converter is introduced and then, its operation principle is analyzed in detail. Switches voltage and current stresses are studied and then, calculation of voltage gain is performed for different states of the converter. Finally, simulation results are given to verify the theoretical analysis and performance of the suggested DC-DC converter.

keywords: *DC-DC converter; Double input; modified Z-source converters; PV/Battery system*

http://dx.doi.org/10.22109/jemt.2018.121505.1069

1. INTRODUCTION

Nowadays, development of power electronic systems for renewable energy applications to obtain efficient and clean energy sources has received more and more interest. Common forms of renewable energy resources include solar and wind energy, hydroenergy, geothermal energy and many of such sources can be employed simultaneously to deliver continuous power to loads. Photovoltaic (PV) is one of the interesting renewable sources due to its clean power generation using the sunlight [1]. This energy has important advantages such as incompleteness, noise-free operation, lack of actuator and mechanical, environmentally friendly and non-contamination. The production of most renewable energy, such as wind and sun, depends on the environmental conditions in various hours of a day and different seasons during a year. Therefore, in energy systems with such energy sources as the main source, the generated power depends on weather conditions. In recent years, the problem of combining such energy sources with other energy sources is considered to improve the reliability of the system. In these systems, energy storage is needed to prevent the reduction or short-term interruptions in power generation. In order to form such hybrid systems, various combinations of sources with energy storage system such as Wind/PV/FC/Battery or PV/FC/Battery systems have been considered.

Some configurations have been introduced for operation of hybrid power systems in which a number of renewable energy sources are connected to a common DC bus through a number of separated single input converters [2, 3]. In such a hybrid power system, to combine the input energy sources with different voltage-current characteristics and generate the intended output voltage, the multi-input converters (MICs) should be employed. Simple structure, high reliability, central control and low building cost are the main advantages of this category of converters [4, 5]. Many researchers have proposed different topologies for DC-DC with emphasis on various subjects such as reduced elements, multi-terminal, high voltage gain, lower voltage and current stresses of elements and so on [6]- [8]. A novel multi-input isolated three-level converter for sustainable energy systems adopting high DC-link voltage is proposed in [9]. A configuration using a combination of a charging switch and a series-connected double-input DC-DC converter (SCDIC) is presented in [10]. The introduced topology scheme uses a combination of a charging switch and a SCDIC. In the case of one port powering or one input being short-circuit, the suggested topology forms a bootstrap circuit with the help of the charging switch and SCDIC switches to charge the powered off port and maintain the expected output voltage, which enhances the reliability of double input conversion, making it robust against one input powering off and fault tolerance against one input short-circuit. Multiple DC sources are integrated to the three-level DC-DC converter, resulting in reduced part-count and allowing flexibility in transformer design and DC-link voltage selection. The proposed architecture eliminates two boost switches which are present in the two-stage counterpart, and enables utilizing low voltage switches. Various multi-input converter based on non-isolated configurations are proposed in [11]. A systematic method for derivation of a multiport converter (MPC) based on the DC-link inductor concept is presented. The MPC is generated by interconnecting multiple pulsating voltage cells (PVCs) through the DLIs. The PVCs can be input type, output type, and bidirectional type, and bidirectional MPC topologies can be harvested if all the PVCs are bidirectional type. A new integrated inverter configuration based on double input DC-DC converter is presented in [1]. Proposed structure of module integrated grid-connected photovoltaic (GPV) is based on double input DC-DC converters. Special structure and switching strategy of the proposed converter result in high efficient power conditioning system for GPVs. The proposed structure of module-integrated GPV uses Dual¬ PV module (DPVM) contains two PVs. A multi-port DC-DC converter for PV/ES power system application is suggested in [12]. Due to application of PV/ES power supply systems in urban places, a high efficiency converter with low number of elements and low generated electromagnetic noise is created. To achieve the mentioned features, soft switching operation is incorporated in the mentioned converter. A special PWM switching strategy is used to achieve soft switching condition in double input operation mode. The converter is able to operate in bidirectional mode, which allows ES to charge and discharge. In [13], configuration synthesis methodology of variety of single-input double-output (SIDO) and double-input single-output (DISO) DC-DC converters with less components number is studied. The principle of topology synthesis states that integrated SIDO and DISO DC–DC converters can be easily developed from conventional SISO converters by replacing a diode with a basic cell inclusive of additional input/output port. The principle is effective for many SISO DC–DC converters, and as an example, topology synthesis based on buck, boost, buck–boost, Cuk, sepic, and zeta SISO converters is performed.

Commonly, the non-isolated MICs are introduced based on structure of the conventional buck or boost DC-DC converters. Due to some special characteristics, Z-source converters (ZSC) were proposed. Advantages of Z-source DC-DC converter over conventional DC-DC converters are less inrush current, improve reliability, and less harmonic injection [14]. A modified Z-source DC-DC converter is proposed in [15], the introduced converter can obtain higher voltage gain with lower voltage stresses of switch and the impedance network capacitor and operate with wide-range load. Therefore, the introduced Z-source DC-DC converter not only has lower cost but also has smaller weight and size. In [16], three typical connection ways between the power source and the impedance network have been concluded. Then different kinds of Z-source DC-DC converter can be obtained by selecting the impedance network type, connection way between the input source and the output load. Application of a Z-source DC-DC converter based on the one-port impedance network, operating in continuous conduction mode (CCM) for PV power generation in a DC microgrid is studied in [17]. A

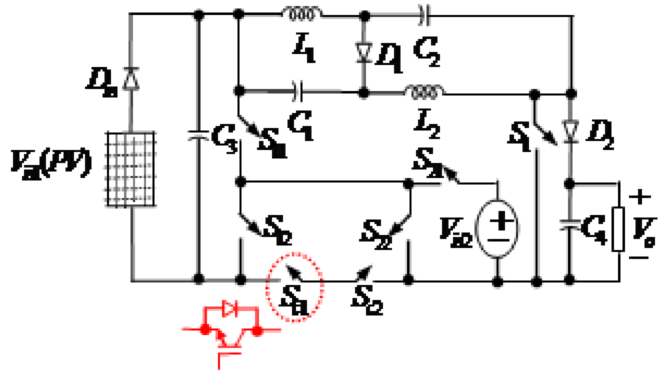

Fig. 1. Configuration of proposed double input Z-source DC-DC converter.

photovoltaic array is connected to the input of ZSC, which provides high voltage gain. In [18], a non-isolated high step-up DC-DC converter which is the derivation of Z-source converter and has a higher voltage gain in comparison to the conventional converters is presented. This advantage makes this converter a suitable choice for photovoltaic applications. Moreover, high boost voltage is obtained with low duty cycle and the energy of leakage inductances is absorbed so the efficiency is increased. In [19], a single stage PV grid integrated modified Z-source inverter is presented. The component sizing, modeling and different modes of operation have been presented. To combine a PV source, a fuel cell source and a battery in a unified configuration, a three-input boost DC-DC converter is presented in [20]. The introduced converter interfaces two unidirectional input power ports and a bidirectional port for a storage element in a unified structure. This converter is interesting for hybridizing alternative energy sources such as PV/FC/battery. Supplying the output load, charging or discharging the battery can be made by the PV and the FC power sources individually or simultaneously. The mentioned structure utilizes only four power switches that are independently controlled with four different duty ratios.

In this paper, a series-connected double input DC-DC converter based on a modified Z-source network is presented. The suggested configuration is suitable for combination of a renewable energy source such as PV unit and battery energy storage system. All operation modes of the converter are analyzed in detail and then, voltage and current stresses of the converter circuit elements are calculated. The converter voltage gain is achieved. Supplementary studies are performed in MATLAB/SIMULINK to verify the performance of the proposed DC-DC converter.

2. PROPOSED CONVERTER CONFIGURATION

Configuration of the proposed double input Z-source DC-DC converter is shown in Fig. 1. The suggested topology consists of passive and active elements including bidirectional switches S_{11}, S_{21}, S_{12}, S_{22}, S_{c1}, S_{c2}, S_1 and two input sources V_{in1} and V_{in2}. The proposed converter can be applied to combine a renewable power sources and battery energy storage system. Indeed, one of the input sources is considered as a backup resource or energy storage during there is no access to the input power source. The topology also has a bootstrap capacitor, C_3. In the converter topology, capacitor C_4 shows filter element, and R_L indicates load resistance. Inductors L_1 and L_2, and capacitors, C_1 and C_2 are impedance network elements.

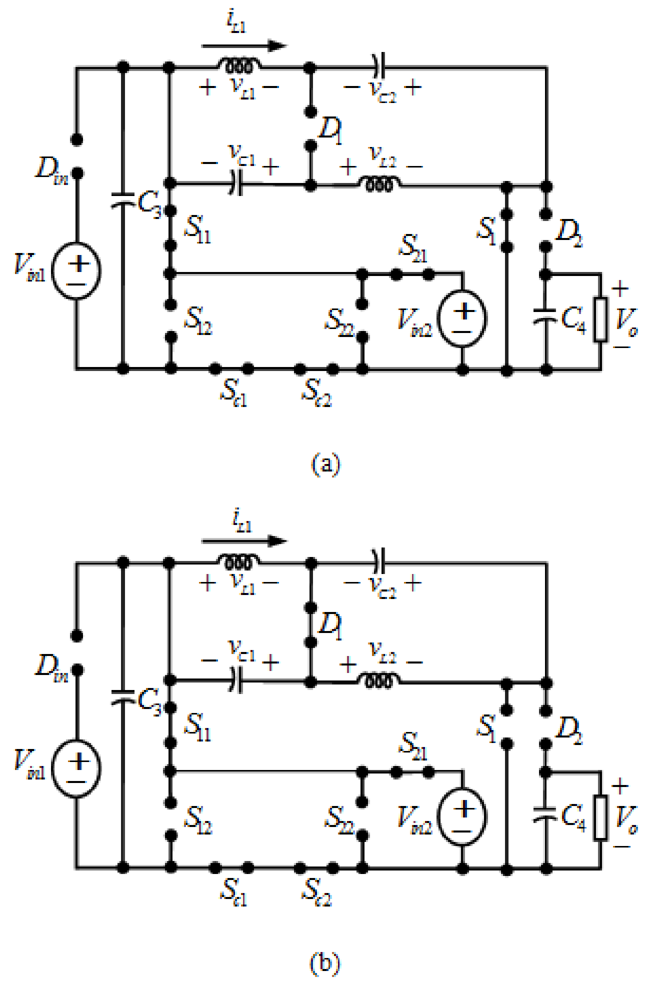

Fig. 2. Converter equivalent circuit in state I (a) first operation mode; (b) second operation mode.

3. PROPOSED CONVERTER OPERATION PRINCIPLE

In steady-state analysis, all elements of converter are assumed to be ideal, the filter capacitor is sufficiently large, and the resistive load is considered at the converter output. Also, in the impedance network, inductors L_1 and L_2, and capacitors C_1 and C_2 are assumed to be equal. The proposed double input DC-DC converter operates in 5 states, and each state has one or two operation modes. D_{SC1} and D_{SC2} are the duty cycle of switches S_{C1} and S_{C2}, and S_{S11}, D_{S12}, D_{S21} and D_{S22} are duty cycles of switches S_{11}, S_{12}, S_{21} and S_{22}. Also, D_{S1} is defined as duty cycle of switch S_1. When one of the input sources is available, two operation states are defined. When the output voltage is greater than either of two input voltages, the duty ratio of switch of the input power unit, S_{21}, should be maximum therefore, in this mode, the switch S_{21} should conduct. The driving signals of switches S_{C1} and S_{C2} are the same as S_{11}.

A. State I (time interval $0 \leq t < t_1$)

In this state, switches S_{11}, S_{21} and S_C conduct, and switches S_{12} and $S_{22}areoff.Fromtwoinputports,only$V$_{in2}$ is connected to the converter. As shown in Fig. 2, the first state includes two operation modes, which are introduced as in the following:

First operation mode ($0 \leq t < t'$): According to Fig. 2(a), in this mode, switch S_1 is on, and diodes D_1 and D_2 are off. For the switch duty cycles greater than 0.5, the converter has negative voltage gain, the polarity of the output voltage is reversed, and the converter operates in the buck/boost mode. For the switch duty cycle less than 0.5, the converter operates in the boost mode. Z-network inductor values are equal therefore, the voltages and currents of these inductors are also equal. The inductor voltage and current are obtained as given in (1)-(4).

$$v_{L1} = V_{in2} + V_{C2} \tag{1}$$

$$v_{L2} = V_{in2} + V_{C1} \tag{2}$$

$$i_{L1} = \left[\left(V_{in2} + V_{C2} \right) \left(t' \right) \right] / L_1 + I_{L1,\min} > 0 \tag{3}$$

$$i_{L2} = \left[\left(V_{in2} + V_{C1} \right) \left(t' \right) \right] / L_2 + I_{L2,\min} > 0 \tag{4}$$

According to (3) and (4), inductors L_1 and L_2 are being charged. Voltages V_{C2} and V_{C1} are the average value of capacitors C_1 and C_2 voltage.

$$i_{C1} = -i_{L1} \tag{5}$$

$$i_{C2} = -i_{L2} \tag{6}$$

According to (4) and (5), capacitors C_1 , C_2 and C_4 are discharged. Actually V_{in2} charged capacitor C_3 and inductors L_1 and L_2.

Second operation mode ($t' \leq t < t_1$): In the second mode, switch S_1 and diode D_2 are turned off, and D_1 is turned on according to Fig. 2(b). The following results are obtained:

In Fig. 2(a) and (b), the power is not transfer from V_{in2} to load however, in these two modes, the voltage source V_{in2} charges the inductors of the impedance network and capacitor C_3.

$$v_{L1} = -V_{C1} \tag{7}$$

$$v_{L2} = -V_{C2} \tag{8}$$

$$i_{L1} = -\left[\left(V_{C1} \right) \left(t_1 - t' \right) \right] / L_1 + I_{L1,\max} < 0 \tag{9}$$

$$i_{L2} = -\left[\left(V_{C2} \right) \left(t_1 - t' \right) \right] / L_2 + I_{L2,\max} < 0 \tag{10}$$

According to (9) and (10), the inductors L_1 and L_2 are discharged. Fig. 2(b) shows that the capacitors C_1, C_2 and $C_3$are charged.

B. State II (time interval $t_1 \leq t < t_2$)

Equivalent circuit of the proposed converter in this state is illustrated in Fig. 3. Switches S_{12} and S_{21} are on and switches S_{11}, S_{22}, S_{C1}, S_{C2} are off. Diodes D_1 and D_2 are on and switch S_1 is off. From Fig. 3, the inductor voltage, v_{L1}, is obtained as given in the following:

$$v_{L1} = V_{in2} + V_{C3} + V_{C2} - V_O \tag{11}$$

$$v_{L2} = V_{in2} + V_{C3} + V_{C1} - V_O \tag{12}$$

The converter boosts the input voltage, so we have:

$$i_{L1} = \left[\left(V_{in2} + V_{C3} + V_{C2} - V_O \right) \left(t_2 - t_1 \right) \right] / L_1 + I_{La} < 0 \tag{13}$$

$$i_{L2} = \left[\left(V_{in2} + V_{C3} + V_{C1} - V_O \right) \left(t_2 - t_1 \right) \right] / L_2 + I_{La} < 0 \tag{14}$$

Therefore, inductors L_1 and L_2 are discharged. From Fig. 3, it is concluded that:

$$v_{L1} = -V_{C1} \tag{15}$$

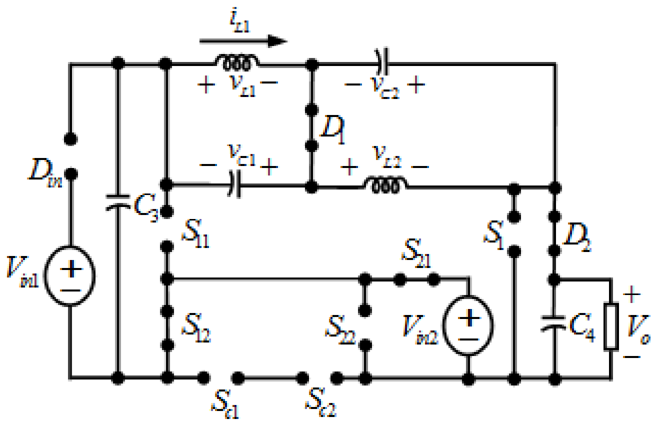

Fig. 3. Converter equivalent circuit in state II.

$$v_{L2} = -V_{C2} \tag{16}$$

$$i_{C1} = i_{L1} - i_{in2} \tag{17}$$

Where, i_{in2} is the current of second input terminal. According to Fig. 3 and (17), the capacitors C_1, $C_2 and C_4$ are charged, and capacitor C_3 is discharged. The voltage and current waveforms of the converter elements in the first and second states of operation is illustrated in Fig. 4.

In this state, voltage source V_{in2} along with capacitor C_3 and impedance network inductors, delivers power to the load.

In this section, operation of the converter when both terminals input power are available is studied. Three different states are defined and described as given in the following.

C. State III (time interval $0 \leq t < t_1$)

In this state, switches S_{12} and S_{21} conduct, and switches S_{11}, S_{22}, S_{C1} and S_{C2} are off. Both input terminals of the converter are involved to deliver power to the DC load. This state has two operation modes. Equivalent circuits of the converter in the modes are illustrated in Fig. 5.

First operation mode ($0 \leq t < t'$): As shown in Fig. 5(a), switch S_1 is on and diodes D_1 and D_2 are off in this mode. The inductor voltage, V_{L1}, and inductors current are determined, as follow:

$$v_{L1} = V_{in1} + V_{in2} + V_{C2} \tag{18}$$

$$v_{L2} = V_{in1} + V_{in2} + V_{C1} \tag{19}$$

$$i_{L1} = \left[\left(V_{in1} + V_{in2} + V_{C1} \right) \left(t' \right) \right] / L_1 + I_{L1\,\text{min}} > 0 \tag{20}$$

$$i_{L2} = \left[\left(V_{in1} + V_{in2} + V_{C1} \right) \left(t' \right) \right] L_2 + I_{L2,\text{min}} > 0 \tag{21}$$

According to (20) and (21), inductors L_1 and L_2 are charged. In this mode, the capacitors C_1 and C_2 are discharged. Also, capacitor C_4 is discharged on the output resistance.

Second operation mode ($t' \leq t < t_1$): As illustrated in Fig. 5(b), diodes D_2 and D_1 conduct and switch S_1 is off. In this mode, the inductor voltage, V_{L1}, and inductors current are achieved as given in the following:

In this state, both sources are active, and in the first mode, voltage sources charge the inductors L_1 and L_2, and then in the second mode, the load power is provided using the inductors discharge.

$$v_{L1} = V_{in2} + V_{in1} + v_{C2} - V_O \tag{22}$$

$$v_{L2} = V_{in2} + V_{in1} + v_{C1} - V_O \tag{23}$$

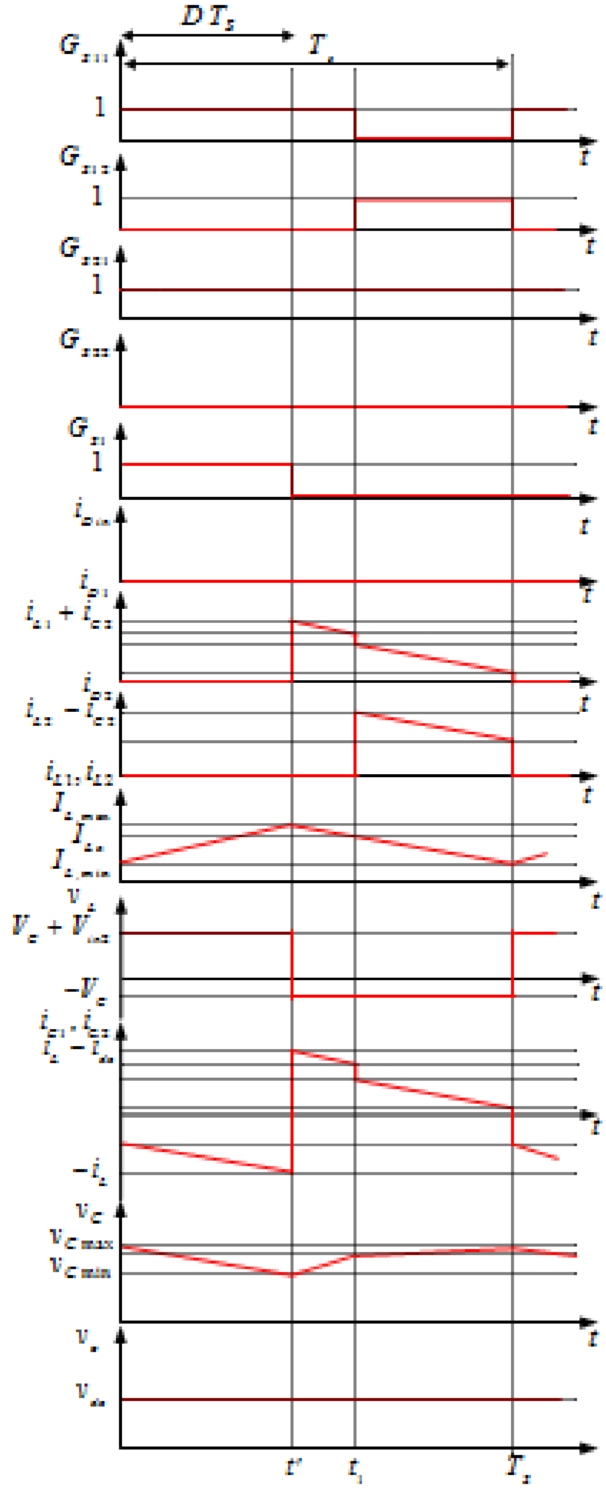

Fig. 4. Voltage and current waveform of important elements of the converter in states I and II.

$$i_{L1} = \left[\left(V_{in2} + V_{in1} + v_{C2} - V_O \right) \left(t_1 - t' \right) \right] / L_1 + I_{L1,\text{max}} < 0 \tag{24}$$

$$i_{L2} = \left[\left(V_{in2} + V_{in1} + v_{C1} - V_O \right) \left(t_1 - t' \right) \right] / L_2 + I_{L2,\text{max}} < 0 \tag{25}$$

Therefore, inductors L_1 and L_2 are discharged. Also, we have:

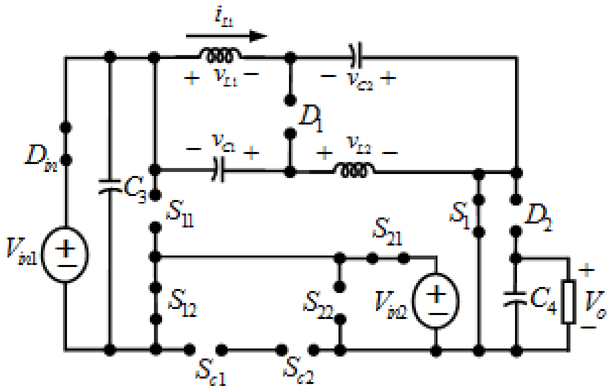

(a)

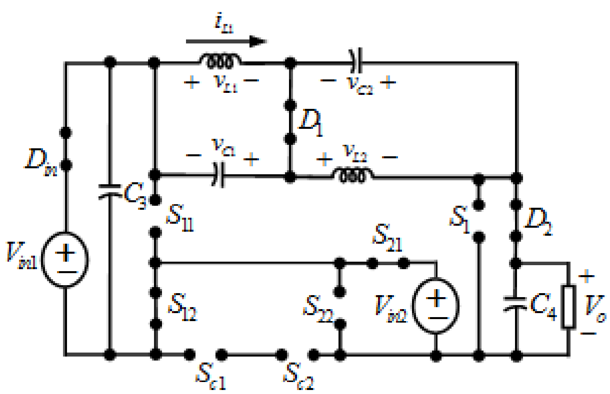

(b)

Fig. 5. Converter equivalent circuit in state III (a) first operation mode; (b) second operation mode.

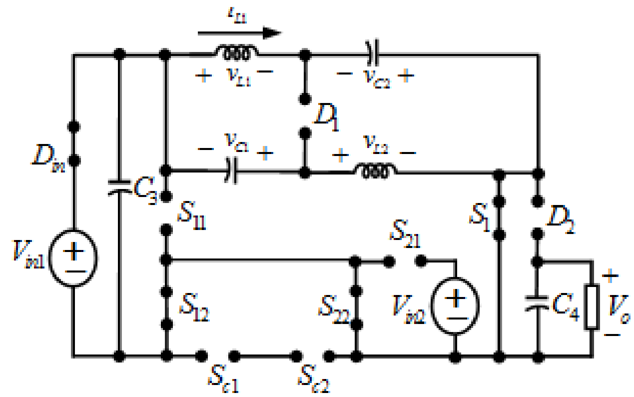

(a)

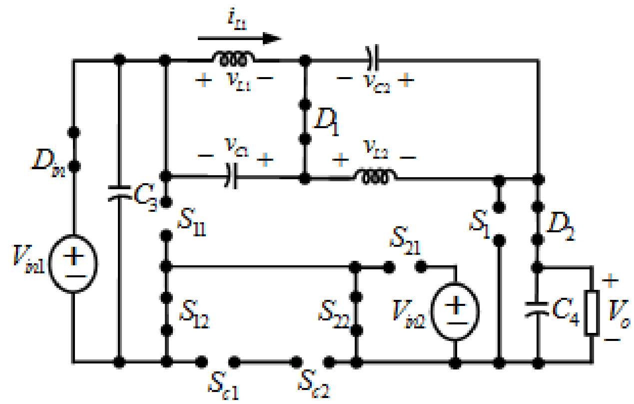

(b)

Fig. 6. Converter equivalent circuit in the state IV (a) first operation mode; (b) second operation mode

$$i_{C1} = i_{L1} - i_{in} \tag{26}$$

$$i_{C1} = \left[\left(V_{in2} + V_{in1} + v_{C2} - V_O\right)\left(t_1 - t'\right)\right]/L_1 + I_{L1,\max} - i_{in} > 0 \tag{27}$$

where i_{in} is the current of the first voltage source. As shown in Fig. 5(b), current of capacitor C_2 is equal to (28).

$$i_{C2} = \left[\left(V_{in2} + V_{in1} + v_{C1} - V_O\right)\left(t_1 - t'\right)\right]/L_2 + I_{L2,\max} - i_{in} > 0 \tag{28}$$

Therefore, capacitors C_1 and C_2 are charged. In this mode, capacitor C_3 is discharged and capacitor C_4 is charged.

D. State IV (time interval $t_1 \le t < T_S$)

In this state, the first voltage source is active. Switches S_{12} and S_{22} conduct and switches S_{11}, S_{21},$S_{C1} and S_{C2}$ are off. This state has two operation modes as shown in Fig. 6. Only the first voltage source is involved to deliver power to the load.

First operation mode ($t_1 \le t < t_2$): As shown in Fig. 6(a), switch S_1 is on and diodes D_1 and D_2 are off in this mode. The inductor voltage, v_{L1}, and inductors current are determined as follow:

$$v_{L1} = -v_{C2} + V_{in1} \tag{29}$$

$$v_{L2} = -v_{C1} + V_{in1} \tag{30}$$

$$i_{L1} = \left[\left(-v_{C2} + V_{in1}\right)\left(t_2 - t_1\right)\right]/L_1 + I_{La} > 0 \tag{31}$$

$$i_{L2} = \left[\left(-v_{C1} + V_{in1}\right)\left(t_2 - t_1\right)\right]/L_2 + I_{La} > 0 \tag{32}$$

The above equations indicate that inductors L_1 and L_2 are charged and capacitors C_1 and C_2 are discharged.

Second operation mode ($t_2 \le t < T_S$): As illustrated in Fig. 6(b), diode D_1 conducts and switch S_1 and diode D_2 are off. In this mode, the inductor voltage, v_{L1}, and inductors current are achieved as given in the following:

$$v_{L1} = -v_{C1} \tag{33}$$

$$v_{L2} = -v_{C2} \tag{34}$$

$$i_{L1} = \left[\left(-v_{C1}\right)\left(T_S - t_1\right)\right]/L_1 + I_{La} < 0 \tag{35}$$

$$i_{L2} = \left[\left(-v_{C2}\right)\left(T_S - t_1\right)\right]/L_2 + I_{La} < 0 \tag{36}$$

According to (35) and (36), inductors L_1 and L_2 are discharged and capacitors C_1 and C_2 are charged. The voltage and current waveforms of the converter elements in the states III and IV is illustrated in Fig. 7.

4. CALCULATION OF CONVERTER VOLTAGE GAIN

Inductor voltage balance law is applied to calculate voltage gain of the proposed converter. For the first and second states according to (1), (7) and (11), the following equation is achieved:

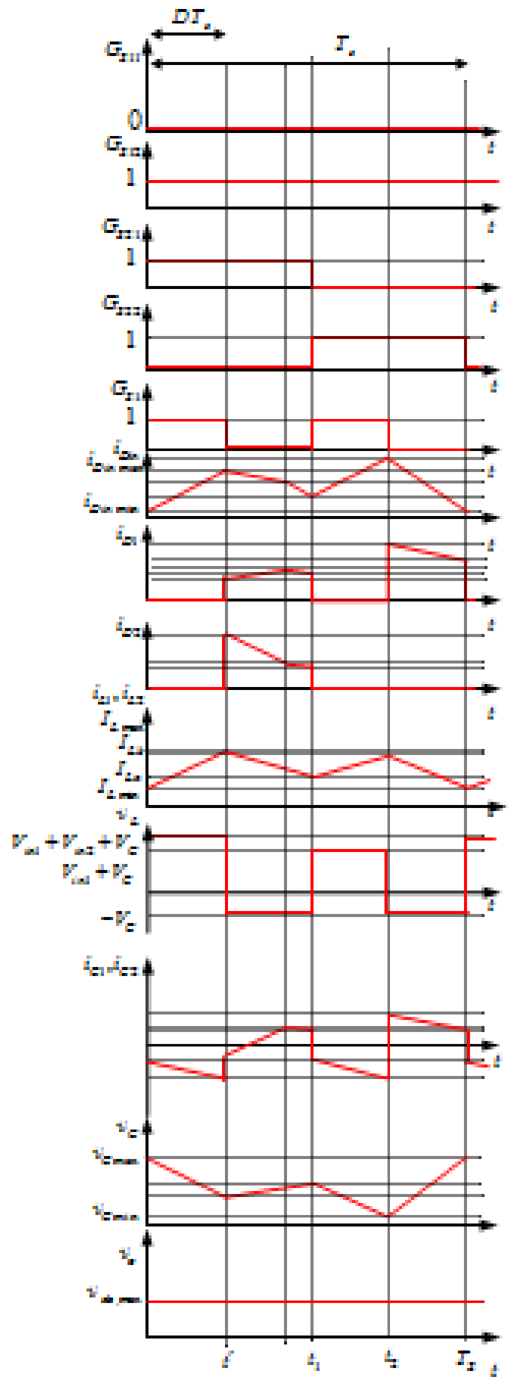

Fig. 7. Voltage and current waveforms of the converter elements in states III and IV.

$$V_{in2}D + V_C(2D-1) = 0 \quad \textbf{(37)}$$

$$V_C = \frac{D}{1-2D}V_{in2} \quad \textbf{(38)}$$

Average value of output voltage is equal to voltage drop across the switch S_1 so, the following equation is obtained:

$$V_O = V_{in2} + 2V_C \quad \textbf{(39)}$$

$$G = \frac{V_O}{V_{in2}} = \frac{1}{1-2D} \quad \textbf{(40)}$$

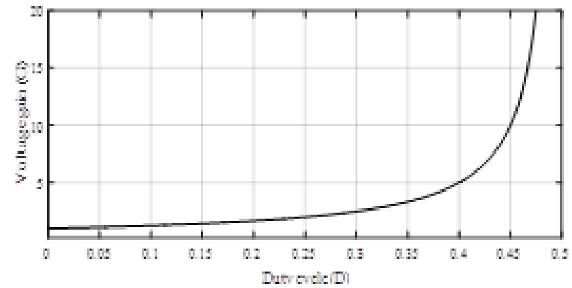

Fig. 8. Voltage gain of proposed converter versus duty cycle in states I&II.

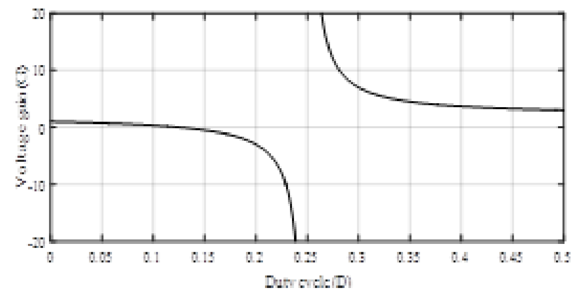

Fig. 9. Voltage gain of proposed converter versus duty cycle in state III.

Similar analysis for state III, when both input sources are available, results in the following equation:

$$(V_{in2} + V_{in1})D + V_C(2D-0.5) = 0 \quad \textbf{(41)}$$

According to (41), the average value of the capacitor voltage is determined as given in the following:

$$V_C = \frac{D(V_{in2}+V_{in1})}{(0.5-2D)} \quad \textbf{(42)}$$

$$V_C = \frac{(-V_{in2}-V_{in1}+V_O)}{2} \quad \textbf{(43)}$$

The converter voltage gain in the mentioned condition is achieved as follows:

$$G = \frac{V_O}{V_{in1}+V_{in2}} = \frac{1-8D}{1-4D} \quad \textbf{(44)}$$

Fig. 8 and Fig. 9 show the voltage gain of the converter versus the duty cycle in states I&II and state III, respectively.

5. CALCULATION OF VOLTAGE AND CURRENT STRESSES OF ELEMENTS

In different modes, with regard to turning off and turning on of different switches, voltage and current stresses of elements are calculated. To obtain the maximum voltage across the switch S11 in the states III and IV, we have:

$$V_{S11(\max)} = V_{in1} \quad \textbf{(45)}$$

Similarly, in state I, to obtain the maximum voltage across the switch S12, we have:

$$V_{S12(\max)} = V_{in2} \quad \textbf{(46)}$$

Also, in state IV, the maximum voltage across the switch S21 is equal to maximum voltage across the switch S22 in the state III.

$$V_{S21(\max)} = V_{S22(\max)} = V_{in2} \quad (47)$$

In the same way, in states II, III (second mode), IV (first mode), the maximum voltage is obtained as given in the following:

$$V_{S1(\max)} = V_O \quad (48)$$

In the states II, III and IV, the maximum voltage across switches SCS1 and SSC2 is determined as given in the following:

$$V_{SC1(\max)} = V_{SC2(\max)} = \frac{V_{in2}}{2} \quad (49)$$

In all of the states, the maximum voltage across diode D1 is zero.

$$V_{D1(\max)} = 0 \quad (50)$$

In states I, III (first mode) and IV, the maximum voltage across diode D2 is calculated as follows:

$$V_{D2(\max)} = V_{in1} + V_{in2} + V_{C2} - V_{L1} - V_O \quad (51)$$

The maximum voltage across diode Din in states I and II is achieved as follows:

$$V_{Din(\max)} = V_{in1} - V_{C3} \quad (52)$$

In state I, maximum current flow through the switch S11 is equal to maximum current of switches S12 and S21 in states II and III. In addition, maximum current flow through the switch S1 in state I (first mode) and state III (first mode) is obtained as given in the following:

$$I_{S11(\max)} = I_{S12(\max)} = I_{S21(\max)} = I_{S1(\max)} = I_{in2} \quad (53)$$

Similarly, switches SSC1 and SSC2 maximum currents in state I are determined as given in the following:

$$I_{SC1(\max)} = I_{SC2(\max)} = I_{in2} - 2I_L \quad (54)$$

As the same way for diodes, in the states I (second mode), II, III (second mode), IV (second mode), the maximum current flow through the diode D1 is calculated as follows:

$$I_{D1(\max)} = I_L + I_C = 2I_L \quad (55)$$

Likewise for diode D2 in state II and III (second mode), the maximum current is determined as given in the following:

$$I_{D2(\max)} = I_L - I_C = I_{in2} \quad (56)$$

For input diode, Din, in state IV and III, the maximum current is equal to (57).

$$I_{Din(\max)} = I_{in1} \quad (57)$$

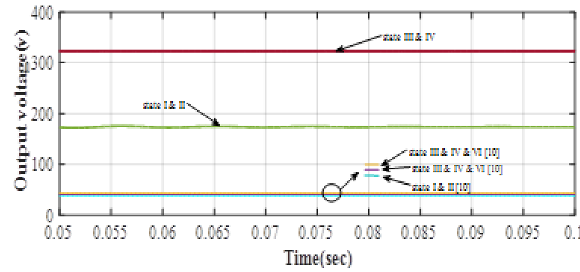

Fig. 10. Comparison of various operation states output voltage of proposed converter with converter presented in [10] for identical input voltages.

6. CALCULATION OF VOLTAGE RIPPLE

To calculate appropriate value for capacitor C4, the passable range for voltage ripple across the capacitor, XC%, is determined as follows:

$$X_C\% = \frac{\Delta v_C}{V_C} \times 100 \quad (58)$$

$$\frac{\Delta v_C}{V_C} = \frac{D}{RC} \quad (59)$$

When the second source is available, the capacitor voltage ripple equals to the output voltage ripple, which is obtained using (54). Meanwhile, when both of sources are available, output voltage ripple achieved as follows:

$$\frac{\Delta v_C}{V_C} = \frac{t_1}{RC} \quad (60)$$

7. COMAPARISON STUDY

operation of proposed double input DC-DC converter is similar to a double input DC-DC presented in [10]. However, their difference in configuration is considerable. Therefore, the mentioned converters are compared in boosting the voltage for identical input voltages, and in various operation states efficiency. It should be noted that the converters are different in circuit elements number and configuration so, the comparisons based on this factors are not possible. For 50V in the first input voltage source and 30V in the second input voltage source, the steady state output voltage waveforms of two converters are given in Fig. 10. Unlike the double input DC-DC converter presented in [10], the proposed double input DC-DC converter has the capability of boosting the voltage such that for 50V and 30V input voltages, the output voltage is 175V in states I and II, and 323V in states III and IV. While, the converter presented in [10] produces 49V output voltage for the same input voltages.

The efficiency of the proposed converter have been tested in MATLA/SIMULINK and given in Fig. 11. Also, the efficiency of presented converter in [10] for various operation states is shown in Fig. 12. It should be noted that in general, the double input converters has lower efficiency than single input converters because of more elements in their structure and different operation. Anyway, results show that the proposed converter has higher efficiency than the presented converter in [10] in most operation states.

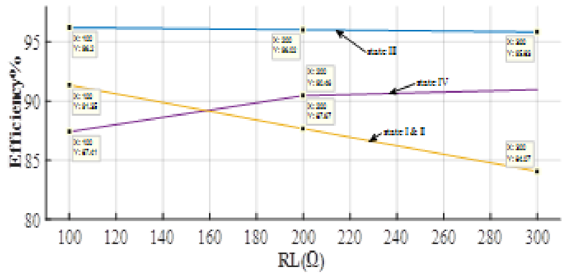

Fig. 11. Efficiency variation of proposed converter for various operation states.

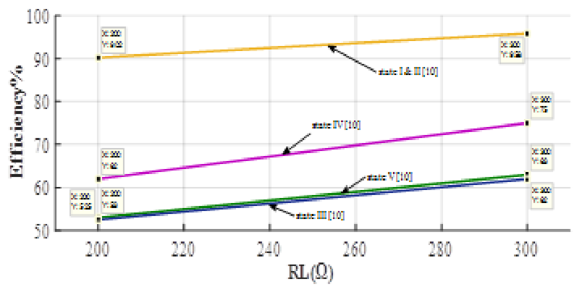

Fig. 12. Efficiency variation of presented converter in [10] for various operation states.

8. SIMULATION RESULTS

To verify the proper operation of proposed double input DC-DC converter, the converter operation is simulated in MATLAB/SIMULINK. Table 1 gives values of the converter elements and parameters. In this study, values of D_{s11}, D_{S12},D_{S21}, D_{S22}, D_{SC1}, D_{SC2} for first and second states are 0.67, 0.33, 1, zero, 0.67 and 0.67, respectively. Considering that the proposed converter operates as a step up converter, it is necessary that the D_{S1} should be less than 0.5. Duty cycle for switch S_1 is equal to 0.4. Fig. 13 shows the waveforms of the proposed converter parameters in the states I and II. Also, capacitors and inductors charging and discharging currents are shown in detail. In state I, switches S11, S21 and SC conduct, and switches S12 and S22 are off. From two input voltage sources, only Vin2 is connected to the converter. The first state consists of two modes. In this figure, charging process of the impedance network elements using Vin2 voltage source in first half switching cycle and discharging process of the energy to the load in the next half switching cycle is shown in detail. In the first mode, the Z-source inductors are charged using Vin2 voltage source and in the second mode, the Z-source inductors charge the capacitors. In the state II, the whole energy from Z-source elements are transferred to the load. As shown in this figure, output voltage is stepped up to 175V using converter impedance network.

For states III and IV, values of D_{s11}, D_{S12},D_{S21}, D_{S22}, D_{SC1}, D_{SC2} are zero, 1, 0.5, 0.5, zero and zero, respectively. Fig. 14 shows the waveforms of the converter parameters in state III and IV. In the first two modes, the Z-source inductors are charged using both two voltage sources and then, the Z-source inductors charge the capacitors and transfer the power to the load. In the second two modes, the Z-source inductors are charged using Vin1 voltage source and then, the Z-source inductors charge the capacitors and transfer the power to the load. As shown in this figure, the output voltage is stepped up to 323V.

Table 1. Parameters Values in Simulation

V_{in1}	50V
V_{in2}	30V
C_1, C_2	100μF
R	300 Ω
(S1) f_s	100KHz
C_3	0.5mF
C_4	0.1mF

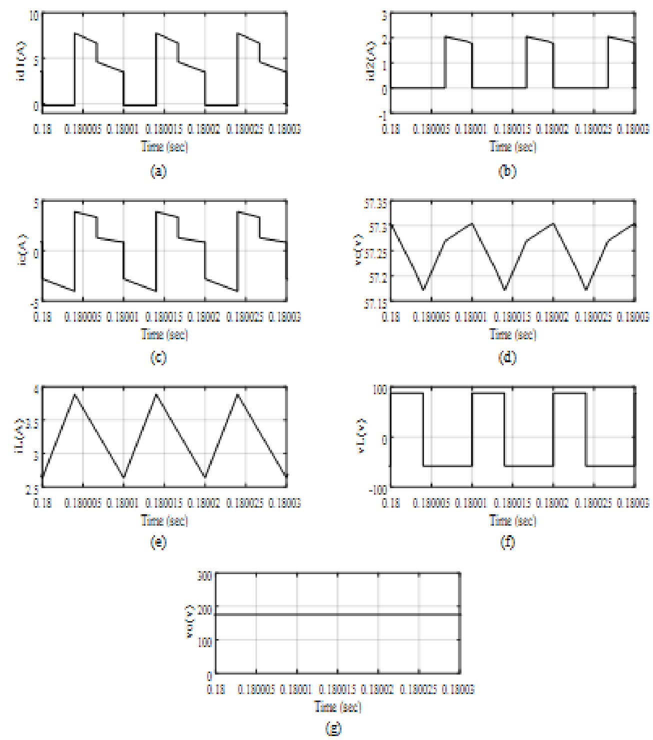

Fig. 13. Waveforms of the proposed converter parameters in states I and II; (a) diode D1 current;(b) diode D2 current; (c) capacitors C1 and C2 current; (d) voltage across capacitors C1 and C2; (e) inductors L1 and L2 current; (f) voltage across inductors L1 and L2; (g) output voltage.

Simulation results show the proper performance of the proposed double input DC-DC converter in delivering the power from two input sources to the output port. As the results show, the converter can absorb the power from each input port individually or from the both ports simultaneously. Moreover, the capability of the proposed converter in boosting the input voltage is indicated in the simulation results.

9. CONCLUSION

A new configuration for double input DC-DC converters based on modified Z-source converter is suggested in this paper. Different operation modes of the proposed converter are completely analyzed and then, the voltage gain, current and voltage stresses, voltage ripple are calculated. The main merits of the suggested

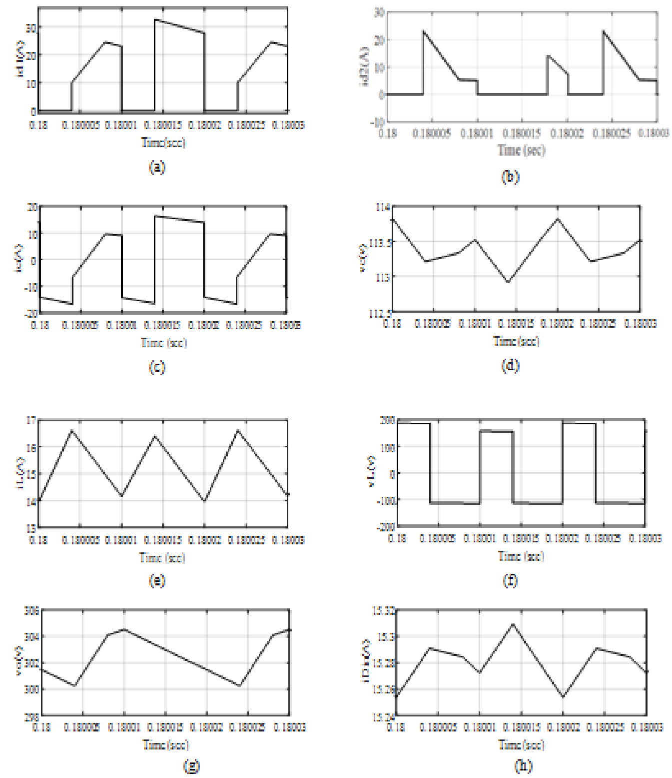

Fig. 14. Waveforms of the proposed converter parameters in state III and state IV, if the first input source, is active; (a) diode D1 current;(b) diode D2 current; (c) capacitors C1 and C2 current; (d) voltage across capacitors C1 and C2; (e) inductors L1 and L2 current; (f) voltage across inductors L1 and L2; (g) output voltage; (h) input current ripple.

converter are its high voltage gain and lower ripple in output voltage. In addition, the studied characteristics of the proposed double input DC-DC converter make it suitable for standalone PV/Battery system application. Simulation results of the suggested converter in MATLA/SIMULINK validate its performance. The results show ability of the proposed double input converter in delivering power from each input voltage source individually or simultaneously. The results indicate that in states I and II, the input voltage is boosted to 175V, and in states III and IV, the input voltage is boosted to 323V. Efficiency of the proposed converter is tested for various load in all of the states.

REFERENCES

1. M. mohammadi, N. Safari, J. milimonfared and J. S. Moghani, “Application of a New High Step-up Double-Input Converter in a Novel Module-Integrated-Inverter Photovoltaic System,” IEEE Conferences (PEDSTC), 27 April 2015.

2. F. Iannone, S. Leva, and D. Zaninelli, “Hybrid photovoltaic and hybrid photovoltaic-fuel cell system: Economic and environmental analysis,” in Proc. IEEE Power Eng. Soc. Gen. Meeting, pp. 1503–1509, 2005.

3. Z. H. Jiang, “Power management of hybrid photovoltaic-fuel cell power systems,” in Proc. IEEE Power Eng. Soc. Gen. Meeting, pp. 1–6, 2006.

4. S. Daniyali, S. H. Hosseini and G. B. Gharehpetian, “New extendable single-stage multi-input dc–dc/ac boost converter,” IEEE Trans. Power Electron, 29, (2), pp. 775–788, 2014.

5. H. Keyhani and H. A. Toliyat, “A ZVS single-inductor multi-input multi-output dc-dc converter with the step up/down capability,” Proc ECCE, Denver, USA, pp. 5546–5552, 2013.

6. V. P. Galigekere, and M. K. Kazimierczuk, “Analysis of PWM Z-Source DC-DC Converter in CCM for Steady state,” IEEE Transaction on Circuits and Systems-I: Regular Paper, Vol.59, no.4, pp.854-863, April-2012.

7. K. Subramanian and V. Kavitha, “Simulation study of double input z-source DC-to-DC converter,” Renewable Energy and Sustainable Energy (ICRESE), 2013 International Conference on, pp. 124-127, 5-6, India, Dec. 2013.

8. F. Sedaghati, E. Babaei, “Double Input Z-Source DC-DC Converter”, IEEE 2nd Power Electronics, Drive Systems and Technologies Conference (PEDSTC), Tehran, Iran, February 2011.

9. S. Dusmez, X. Li, and B. Akin, “A New Multi input Three-Level DC/DC Converter,” IEEE Trans. on Power Electronics, Vol. 31, No. 2, pp. 1230-1240, Feb. 2016.

10. X. Sun, Y. Zhou, W. Wang, B. Wang, and Zh. Zhang, “Alternative Source-Port-Tolerant Series-Connected Double-Input DC–DC Converter,” IEEE Trans. On Power Electronics, Vol. 30, No. 5, pp. 2733 – 2742, 2015.

11. H. Wu, J. Zhang, Y. Xing, “A family of multi-port buck-boost converters based on DC-link-inductors (DLIs),” IEEE Trans. Power Electron, vol. 30, no. 2, pp. 735–746, Feb. 2015.

12. M. mohammadi, J. milimonfared, M. R. M. Behbahani and J. S. Moghani, “A Double-Input Converter for Hybrid Supply Systems,” IEEE Conferences (PEDSTC), 27 April 2015.

13. G. Chen, Z. Jin, Y. Deng, X. He and X. Qing, “Principle and Topology Synthesis of Integrated Single-Input Dual-Output and Dual-Input Single-Output DC-DC Converters,” IEEE Tans. On Indusrtial Electronics, Vol. pp, 2017.

14. F. Z. Peng, “Z-source inverter,” Industry Applications Conference. 37th IAS Annual Meeting, vol. 2, pp. 775 - 781, 2002.

15. L. Yang, D. Qiu, B. Zhang, G. Zhang, W. Xiao, “A Modified Z-Source DC-DC Converter,” School of Electric Power, South China University of Technology IEEE Power Electronics and Applications (EPE’14-ECCE Europe), 2014 16th European Conference on.

16. D. Qiu, B. Zhang, L. Yang, G. Zhang and F. Xie, “Study on the construction method of Z-source DC-DC converters,” 2016 IEEE 7th International Symposium on Power Electronics for Distributed Generation Systems (PEDG), pp. 1-6, Canada, August 2016.

17. L. A. De Castro, F. L. M. Antunes, E. M. Sa, “DC-DC Z-source Converter Applied to PV System,” Power Electronics for Distributed Generation Systems (PEDG), Florianopolis, Brazil, 2017 IEEE 8th International Symposium on.

18. A. Torkan, M. Ehsani, “High step-up Z-source DC-DC converter with flyback and voltage multiplier,” IEEE Applied Power Electronics Conference and Exposition (APEC), Tampa, FL, USA, 2017.

19. S. A. Singh, G. Carli, N. A. Azeez, and S. S. Williamson, “A Modified Z-source Converter based Single Phase PV/Grid Inter-connected DC Charging Converter for Future Transportation Electrification,” Energy Conversion Congress and Exposition (ECCE), Milwaukee, WI, USA, 2016.

20. F. Nejabatkhah, S. Danyali, S. H. Hosseini, M. Sabahi, and S. M. Niapour, “Modeling and control of a new three-input dc-dc boost converter for hybrid PV/FC/battery power system, ” IEEE Trans. Power Electron., vol. 27, no. 5, pp. 2309–2324, May 2012.